

УДК 533.9.01

GENERATION OF A HOMOGENEOUS ARGON PLASMA COLUMN IN BEENAKKER CAVITY**A.V. TATARINOV¹, I.L. EPSTEIN¹, M. GAVRILOVIĆ², S. JOVICEVIĆ²,
N. KONJEVIĆ³, Yu.A. LEBEDEV¹**¹ *Topchiev Institute of Petrochemical Synthesis RAS, Moscow, E-mail: lebedev@ips.ac.ru*² *Institute of Physics, University of Belgrade, Belgrade, Serbia,*³ *Faculty of Physics, University of Belgrade, Belgrade, Serbia***ГЕНЕРАЦИЯ ОДНОРОДНОГО ПЛАЗМЕННОГО СТОЛБА В АРГОНЕ В РЕЗОНАТОРЕ
БЕЕНАККЕРА****А.В. ТАТАРИНОВ¹, И.Л. ЭПШТЕЙН¹, М. ГАВРИЛОВИЧ², С. ЙОВИЧЕВИЧ²,
Н. КОНЕВИЧ³, Ю.А. ЛЕБЕДЕВ¹**¹ *Институт нефтехимического синтеза им. А.В. Топчиева РАН, г. Москва,*² *Институт физики Белградского университета, г. Белград, Сербия,*³ *Физический факультет Белградского университета, г. Белград, Сербия***Summary**

Long homogeneous column of argon plasma at a pressure of 0.5 Torr, generated by means of the Beenakker cavity, has been investigated by methods of emission spectroscopy, photography and self-consistent 3D modeling in a nonlocal approximation.

Key words: homogeneous plasma, argon, ionization zone, rotational structure of the spectra.

Аннотация

Протяженный столб однородной плазмы в аргоне, полученный в микроволновом резонаторе Бее-наккера исследован методами эмиссионной спектроскопии, фотографирования и самосогласованного 3D моделирования в нелокальном приближении.

Ключевые слова: однородная плазма, аргон, Beenakker cavity, nonlocal approximation.

1. Experiments and measurement procedure

Design and dimensions of the resonator and the sketch of spectral measurements are shown in Fig. 1a. Quartz tube passes through the axis of symmetry of the resonator. An argon discharge is ignited inside the quartz at a pressure of 0.5 tor and gas flow of 0.2 l/min. The external parts of the tube outside the resonator are equal in length.

The resonator is excited by a coaxial feeder with inner rod antenna, vertically entered through the top cover of the cavity ($f = 2.45$ GHz, $P_{inc} = 80$ W). Optical emission of the discharge is registered with the digital camera and spectrometer.

The discharge emission is uniform both along the length of the column and when collected at the end of the quartz tube (Fig. 1b). However the "end-on" and "side-on" temperatures determined by the intensity of emission of excited p and d states of argon atoms collected at the end and perpendicular to the discharge tube were found quite different: 1900-2200 K and 4350-4900 K respectively. Explanation for such a difference in temperatures has been found due to the simulations.

2. Modeling of the discharge

Since the electrodynamic system with the energy feeder and tuning rod is asymmetric, one needs a three-dimensional model. The model contains the Maxwell equations, Poisson equation and kinetic equations for the

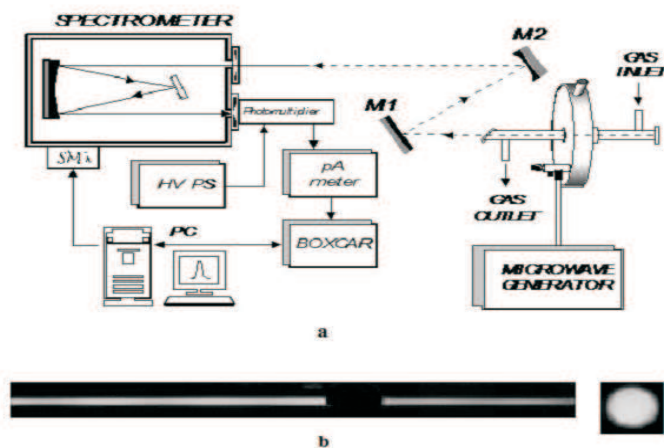


Fig. 1: a – the scheme of end-on measurement of emission spectra of argon discharge in the Beenakker's cavity; b – photo of a discharge in argon, dark gap corresponds to the cavity; photo of the discharge at the end (right)

electrons, argon ions (Ar^+ and Ar_2^+) and electronically excited argon states: coupled metastable $^3\text{P}_2 \dot{-} ^3\text{P}_0$ level $\text{Ar}(\text{M})$, coupled resonant $^3\text{P}_1 \dot{-} ^1\text{P}_1$ level $\text{Ar}(\text{R})$ and 3 higher lying lumped levels $\text{Ar}(\text{F})$, $\text{Ar}(\text{A})$, $\text{Ar}(\text{B})$ [2]. The model includes the following processes: direct and stepwise electron excitation of Ar; interchange of metastable and resonant states under the electron impact; emission of higher lying argon states; dissociative recombination of Ar_2^+ ion; wall quenching of the excited argon states.

The processes of chemi-ionization with generation of ions Ar^+ and Ar_2^+ , i.e., $\text{Ar}(\text{M}) + \text{Ar}(\text{M}, \text{R}) \rightarrow \text{Ar}^+ + \text{Ar} + e$ and $\text{Ar}(\text{M}) + \text{Ar}(\text{M}, \text{R}) \rightarrow \text{Ar}_2^+ + e + e$ were included in the kinetic scheme.

We also took into account the reabsorption when calculating the loss of resonant state of $\text{Ar}(\text{R})$ and higher lying lumped level $\text{Ar}(\text{F})$ due to emission.

A nonlocal approximation is used for a description of the discharge [3]. In this case the local link of parameters of the electronic component with microwave field is absent, it is replaced by the balance equation of the electron energy density [4, 5].

The model contains pre-computed table files with the rate constants of reactions which include an electron impact. The electron energy distribution functions, needed for calculation of those constants, have been obtained by solving the Boltzmann equation for the free electrons of the plasma in the two-term approximation.

The plasma and wave equations are solved numerically, using finite element methods implemented in the commercial package Comsol 3.5a [6].

2. Results and discussion

Simulations showed that the plasma can be divided into two areas: a central ellipsoidal core, located mainly inside the resonator and projecting slightly beyond it, and peripheral homogeneous column uniformly filling the quartz tube outside the resonator. The microwave field concentrates mostly inside the resonator with maximal values at the walls of the quartz tube. Outside the resonator the wave decays at a distance of a few millimeters. The characteristic peaks of stationary field (Fig. 2a) outside the resonator's cavity correspond to a local resonant increase of the field. In contrast to the microwave field the mean electron energy (Fig. 2b) does not vanish at the exit of the resonator's cavity, it is set constant and equal to about 3 eV. In the central region the mean electron energy on the axis is about 3.5 eV. We note that outside the central region the mean electron energy is quite high and kinetic processes, initiated by direct electron impact, make a significant contribution. Such characteristic steady distribution of energy is typical for the nonlocal problem and determines the spatial distribution of all plasma particles.

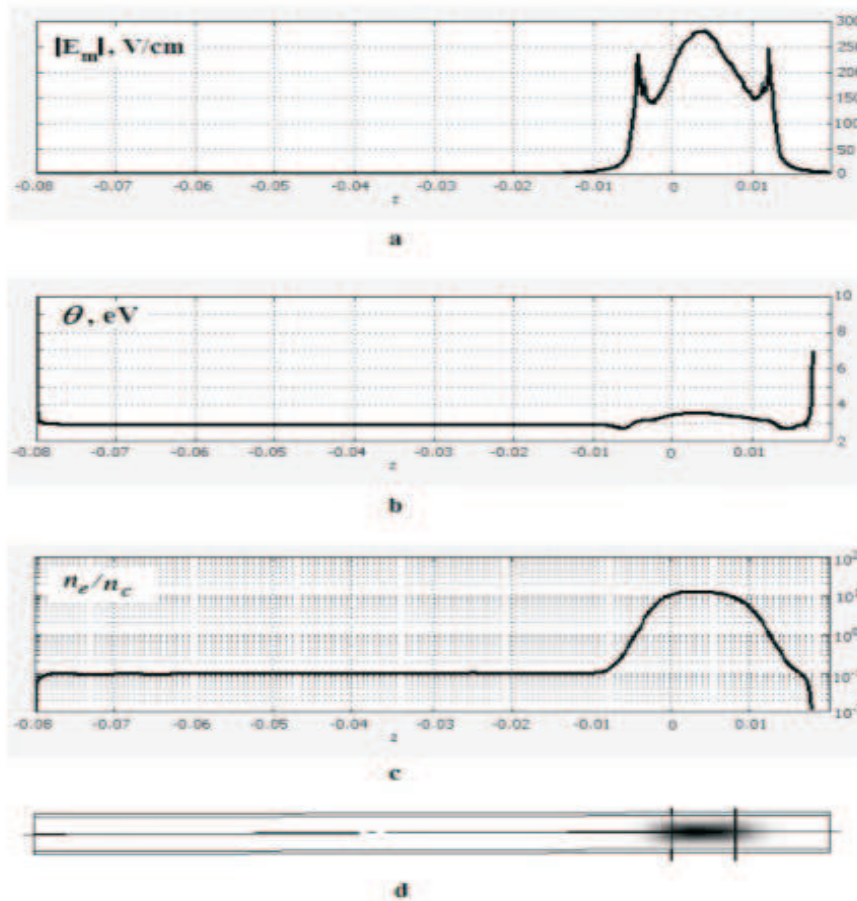


Fig. 2: Profiles of: a – microwave field; b – mean electron energy; c – electron density, along the vertical axis Oz of the tube; d – the electron density diagram on a vertical slice of the tube. Vertical lines correspond to the boundaries of cavity.

The simulations allowed determining of the mechanisms of population of Ar (F, A, B) effective states. It was found that in the central region of the discharge the Ar(F) state is mainly populated due to the stepwise processes and the Ar(A, B) states - by the direct electron impact. In the discharge tube outside the cavity all of these states are populated due to the direct electron impact. According to the simulations these mechanisms lead to an overpopulation of Ar(F) state (13.2 eV) in the central region, compared with the excitation due to only the direct electron impact, and hence to a decrease in temperature. It is the central region of the discharge tube which gives the main contribution during the end-on line intensity measurement collected from the discharge tube. When measuring the side-on intensity of the line emission along the line for collecting the emission, placed close to the resonator's cavity, both the tail of the central core and uniform column contribute to the total collected intensity.

In the simulations the end excitation temperature for p and d states of argon, determined by the line intensities, collected from the end of the discharge tube is found equal to 3600 K. The accuracy of the calculated values is about 50%. As to the side excitation temperature, the total emission intensity will depend on the distance between the line for collecting the emission and the bottom of the resonator's cavity. According to simulations it could vary up to 7000 K.

Simulations have shown that the emission intensity of the excited atoms, collected from the end of the discharge tube, is uniform along the diameter of the tube. They confirmed similar end-on optical measurements

made in the visible spectrum of argon plasma.

REFERENCES

1. **Beenakker C.I.M.** // Spectrochim. Acta. – 1977. – V. 32B. – P. 173.
2. **Dyatko N.A., Ionikh Y.Z. et al.** // J. Phys. D: Appl. Phys. – 2008. – V. 41. – P. 055204.
3. **Kudryavtsev A.A., Smirnov A.S., Tsendin L.D.** Physics of Glow Discharge [Fizika tleushego razrjada]. – St. Petersburg: Lan', 2010. – 512 p. (in Russian)
4. **Shkarofsky I.P., Johnston T.W., Bachynski M.P.** The Particle Kinetics of Plasmas. – Addison-Wesley PC, 1996.
5. **Hagelaar G.J.M., Pitchford L.C.** // Plas. Sources Sci. Technol. – 2005. – V. 14. – P. 722-733.
6. COMSOL 3.5a (<http://www.comsol.com>).